2 Construction and Upgrading of Beamlines

2-1 The Soft X-Ray Capability of the XAFS Station, BL-9A

BL-9A was constructed as a beamline for XAFS experiments using a bending magnet source. A pair of bent conical mirrors is used for collimating and focusing the X-rays and a Si(111) double crystal monochromator is placed between them. Owing to this special optics BL-9A provides high flux (6×10^{11} ph/s at 7 keV, 450 mA) in a 1mm × 1mm area without sacrificing energy resolution [1-4]. The maximum usable photon energy is designed to be 15 keV, limited by the critical angle of the mirrors.

In conventional X-ray beamlines, three 0.2-mm thick beryllium windows are placed between the storage ring and the experimental setup, and the XAFS experiments are carried out under atmosphere. However the transmission of 2.1-keV X-rays (corresponding to the P K-edge) is less than 0.1% due to the presence of the Be windows. Thus most experiments using soft X-rays below 4 keV are carried out under a vacuum environment, limiting the kind of samples and environments available for study and lengthening experiment turn-around times.

Besides the features described above, BL-9A is designed to provide X-rays with energies down to 2.1 keV. In order to realize such performance, the number and thickness of the Be windows is limited; only two 0.1-mm thick Be windows are present in the beamline. Furthermore, a pair of flat mirrors is installed in order to reduce higher order reflections. By using this equipment and a fluorescent ion chamber [5], a XANES spectrum of Ar in air was easily obtained (Fig. 1). However it was not easy to measure XAFS spectra of sulfur or phosphorus with the usual setup owing to the absorption of the X-rays by air. Thus we have constructed a new, simple setup as shown in Fig. 2. The environment between the exit window of the beamline and the sample, including the entrance slit and I0 monitor, is replaced by helium. Since the sample environment is a He atmosphere it is easy to use conversion electron yield (CEY) detection method as well as fluorescent yield (FY) measurements. 700 V is applied to a thin aluminized Mylar film placed before the entrance window of the fluorescence detector and the CEY signal is obtained by directly measuring the sample current.

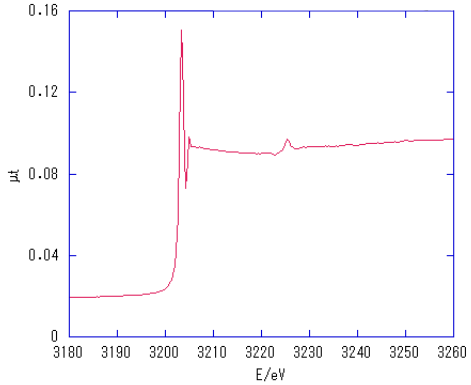

Figure 1
XANES spectrum of Ar in air.

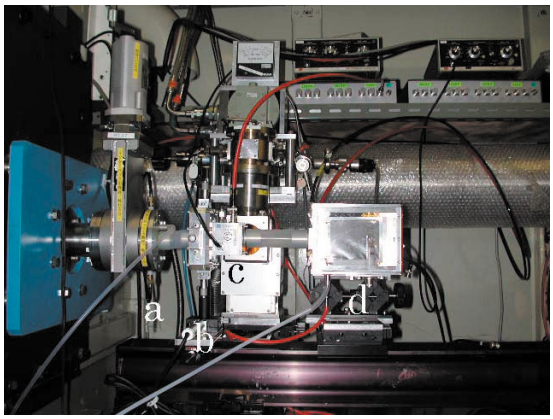

Figure 2
Photograph of the setup for soft X-ray XAFS experiments. a: beam line exit window, b: entrance slit, c: I0 monitor, d: sample chamber.

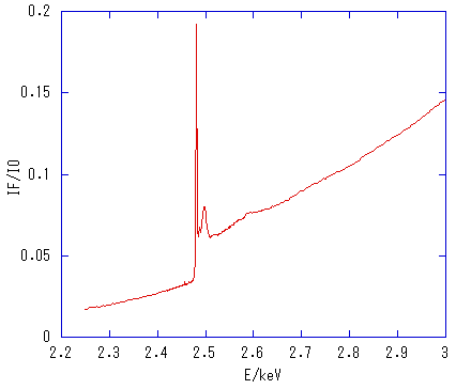

Figure 3
Sulfur K-XAFS spectrum of Scotch tape in FY mode.

Powdery samples are usually rubbed on adhesive tapes. But most commercially available adhesive tapes contain sulfur compounds; an example is shown in Fig. 3. 3M's "Clear Tape" and Nichiban's "Nice tac" showed very little sulfur K-edge thus these tapes were used to support powdery samples in the FY detection mode. On the other hand Scotch Graphite tape AL-25DC was used despite the fact that it contains sulphur for the CEY detection mode in order to realize electrical conductivity. Examples of sulfur XANES spectra can be found in the “Highlights” section (9-1; p. 43).

References

[1] *Photon Factory Activity Report* **1996 #14** (1997) E-5.
[2] *Photon Factory Activity Report* **1999 #17** (2000) A90.
[3] M. Nomura and A. Koyama, *J. Synchrotron Rad.* **6** (1999) 182.
[4] M. Nomura and A. Koyama, *Nucl. Instrum. and Methods Phys. Res. A* **467-468** (2001) 733.
[5] F.W. Lytle, R.B. Greegor, D.R. Sandstrom, E.C. Marques, J. Wong, C.L. Spiro, G.P. Huffman and F.E. Huggins, *Nucl Instrum. Methods Phys. Res.* **226** (1984) 542.

2-2 AR-NW2A, Time-Resolved XAFS Station

As described in the preceding volumes of the Activity Report, AR-NW2A has been designed for both conventional and dispersive XAFS experiments using monochromatic and white X-rays, respectively. Commissioning of the beamline components such as the double crystal monochromator with a liquid nitrogen cooling system, the focusing mirror, and the cut-off mirror system has progressed since February 2002, and is almost complete.

For the conventional XAFS measurements, highly brilliant monochromatic X-rays can be obtained using the bent cylindrical mirror. Figures 4 (a) and (b) show the horizontal and vertical beam profiles measured at the focus-position for several opening sizes of the aperture at 16 m from the source point. The vertical slit size was fixed at 2 mm, *i.e.*, the vertical opening beam divergence was 0.125 mrad. The horizontal slit size was varied with openings of 1.6 mm, 3.2 mm, 4.8 mm and 6.4 mm so as to accept divergences of 0.1, 0.2, 0.3, and 0.4 mrad, respectively. When the horizontal aperture size was increased, a characteristic tail emerged in the vertical profile as shown in Fig. 4(b) because of the aberration of the bent cylindrical mirror. On the other hand, the horizontal profile was less affected. Both the vertical and horizontal beam profiles are consistent with the results of ray-tracing calculations (Fig. 4(c) and (d)). Table 1 summarizes the FWHMs of the focused beam sizes in the vertical and horizontal directions and also the absolute photon fluxes through areas of 0.4 × 0.8 mm^2 and 0.4 × 0.5 mm^2 at the sample position. The photon flux was measured at a monochromatic energy of 12.4 keV using the 3rd harmonics of the undulator synchrotron radiation. Performance is consistent with calculations, and the total flux through an area of 0.4 × 0.5 mm^2 is about 5 × 10^{12} photons/s with a stored current of 50 mA.

Some test XAFS measurements have been performed in both the step-scanning and energy-dispersive modes. Here we introduce a dispersive XAFS (DXAFS) study on a catalytic reaction process as an example. A Cu catalyst supported on zeolite (Cu/ZSM-5) for NOX reduction was prepared and set in the apparatus (shown in Fig. 5). Time-resolved DXAFS spectra were measured during the catalytic reaction process which was initiated by the sudden introduction of a mixed gas of CO (6.9 kPa) and NO (26.6 kPa) at 500°C. Figure 6(a) shows the DXAFS spectra at the Cu K-edge for initial (t = 0 s), intermediate (30-40 s), and final (140-150 s) states and Fig. 6(b) indicates the time dependence of the absorption intensity at 8983 eV (the vertical broken line in Fig. 6(a)). As can be clearly seen in Fig. 6(b), there are two chemical reaction processes taking place. One is a rapid reaction, the creation process of an intermediate state which occurs within several seconds. The other is a slow reaction, where the intermediate state repopulates the initial state over a period of 100-200 s. Figures 6(c) and (d) show DXAFS spectra recorded during these two reaction processes. From these XAFS spectra, it is clear that Cu(II) is reduced to Cu(I) in the intermediate state. Full details of the scientific results obtained by this experiment will be presented elsewhere [1]. It should be emphasized here that each DXAFS spectrum was measured with an exposure time of only 6 ms, but that the statistical accu-

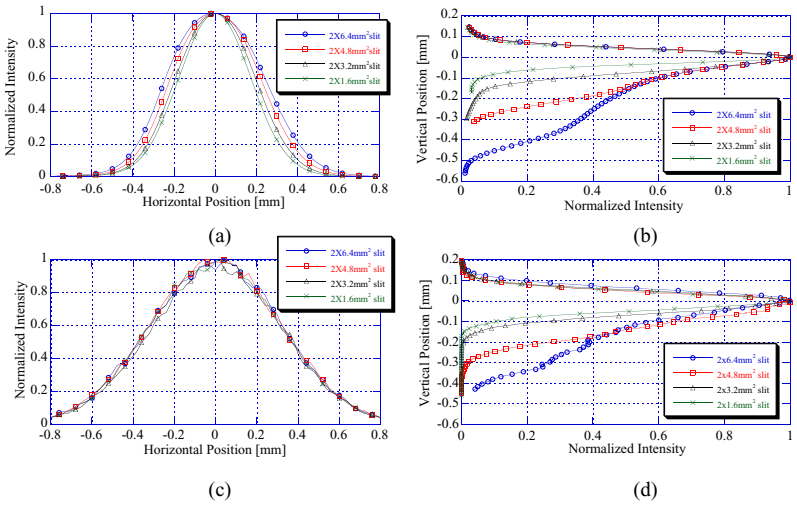

Figure 4
Comparison between the experimentally obtained focused beam profiles (a and b) and those obtained by a ray-tracing calculation (c and d). The opening sizes of the aperture at 16 m from the undulator source are indicated.

Table 1 Quantitative comparison between the real performance and calculation. Inside values of ( ) correspond to the values obtained from ray-tracing calculation.

Size of slit before the focusing mirror (V × H) [mm^2]	Vertical size of focused beam (FWHM) [mm]	Horizontal size of focused beam (FWHM) [mm]	Intensity through the area $0.4^V \times 0.8^H$ mm^2 [$\times 10^{12}$ photons/s]	Intensity through the area $0.4^V \times 0.5^H$ mm^2 [$\times 10^{12}$ photons/s]
2.0 × 6.4	0.21 (0.20)	0.55 (0.74)	6.4 (4.8)	5.3 (3.4)
2.0 × 4.8	0.19 (0.19)	0.50 (0.74)	5.9 (4.8)	4.8 (3.4)
2.0 × 3.2	0.12 (0.13)	0.45 (0.74)	4.0 (3.6)	3.4 (2.6)
2.0 × 1.6	0.08 (0.10)	0.41 (0.75)	2.1 (1.8)	1.7 (1.3)

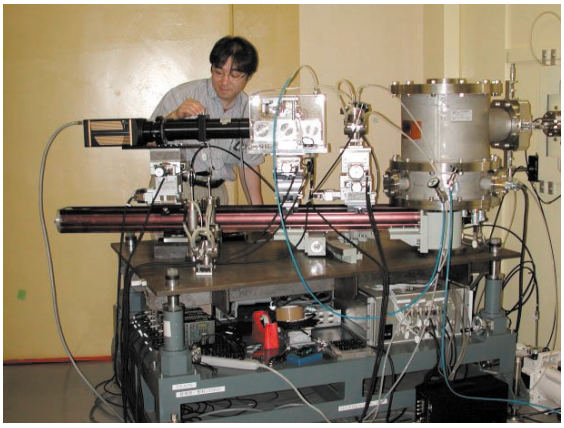

Figure 5
DXAFS apparatus with Dr. Y. Inada of Nagoya University.

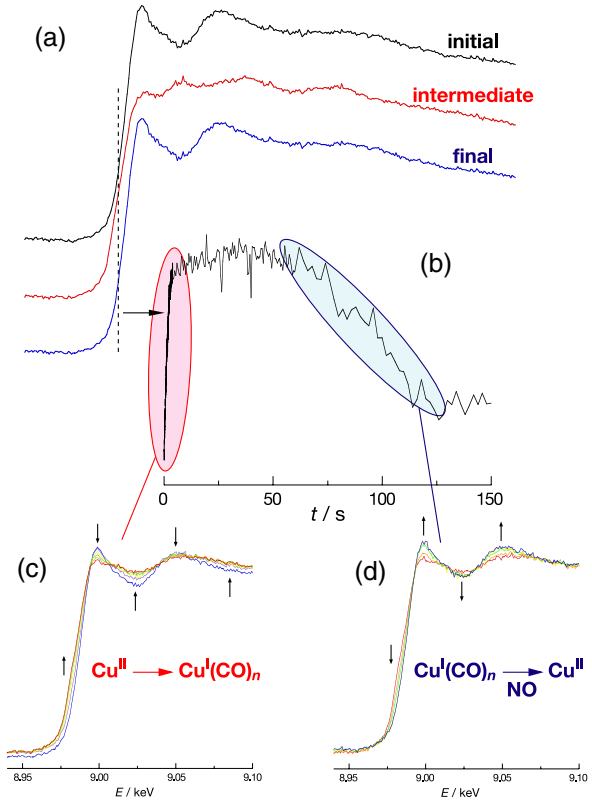

Figure 6
Time-resolved energy-dispersive XAFS spectra recorded during a reaction process of the Cu/ZSM-5 catalyst.

racy is sufficient to investigate catalytic processes. This means that detailed information can be obtained for a non-reversible chemical reaction within several tens of milliseconds. For a reversible chemical reaction, it is in principal possible to observe the reaction on a time scale of 100 ps, the bunch length at the PF-AR. Such studies are the main scientific subject for this beamline.

The commissioning has also begun of a new experimental apparatus for time-resolved diffraction experiments to reveal the structural changes of many interesting materials in photo-induced phase transition technique. The first pump and probe measurements will be carried out in the beginning of 2004.

References

[1] Y. Inada and M. Nomura, to be published.

2-3 AR-NW12A, Protein Crystallography Beamline

AR-NW12A is a new protein crystallography beamline at the PF-AR designed for high-throughput MAD experiments. Construction was completed in FY2002, and the first beam observed on September 30, 2002. After commissioning of the beamline components, NW12 will be opened for public use in May 2003.

For high-throughput MAD experiments, both high beam intensity and good energy tunability are required. To meet these requirement, the beamline was designed with the following specifications.

1) An in-vacuum tapered undulator is used as the source, providing high-flux X-ray beam optimized at around 12.7 keV using the 3rd harmonics.

2) A bent-flat collimating mirror and a liquid nitrogen circulation system for cooling the monochromator crystals are used to achieve good energy resolution.

3) The monochromator, which consists of double flat Si(111) crystals, covers a wide energy range from 7 to 17 keV with a fixed beam exit mechanism.

4) A bent-cylindrical mirror focuses the beam onto the sample position in both the horizontal and vertical directions. The location of the mirror is chosen to realize 2:1 focusing, and hence reduce the beam divergence.

Figure 7 shows a plan view of the beamline. The front-end consists of a fixed mask, a beam-position monitor, an absorber, a beam shutter, a graphite heat absorber, XY-slits for white X-rays and Be windows. The location and the specification of the main optical components are

Table 2 Specification of the optical components.

Insertion device	Type: tapered undulator Length of period: 40 mm Number of periods: 95 Magnetic field: max 0.6Tesla Energy range: 7-17 keV with the 3rd harmonics
Collimating mirror (23.5 m from the source)	Type: bent-flat Material: Rh-coated Si single crystal Size (mm): 1000(L) x 100(W) x 70(T) Glancing angle: 3.5 mrad Radius of curvature: 13428.6 m Slope error(urad): max. 1.56 (L), 5.71(W) Roughness: max. 1.34A
Double crystal monochromator (25.4 m)	Material: Si(111) Fixed exit: numerical link Cooling system: liquid nitrogen circulation Energy range: 7 – 17 keV
Focusing mirror (27.0 m)	Type: bent-cylindrical Material: Rh-coated Si single crystal Size(mm): 1000(L) x 100(W) x 70(T) Radius of curvature: 54.76 mm, 6285.7 m Glancing angle: 3.5 mrad Slope error(urad): max. 3.37(L), 5.93(W) Roughness: max. 1.61A

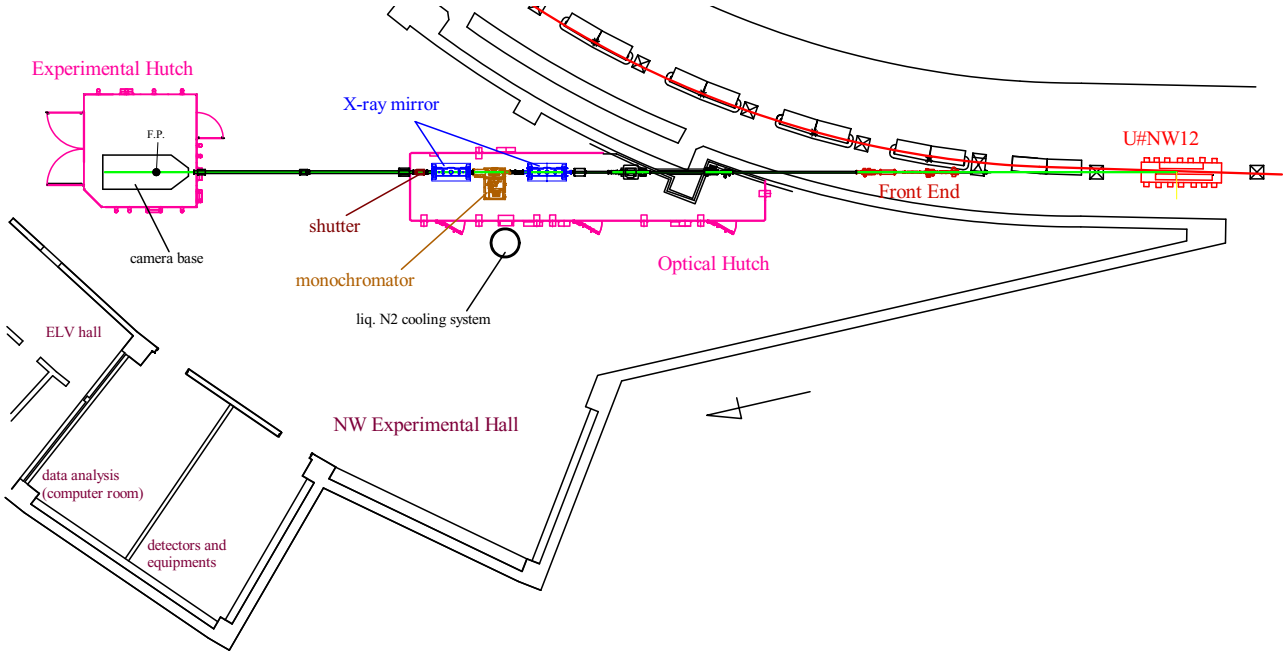

Figure 7
Plan view of the AR-NW12A.

summarized in Table 2. The specifications of the undulator and the monochromator are almost the same as those installed in AR-NW2A, a detailed description of which was given in the preceding volume of the Activity Report [1].

Figure 8 shows the deviation of the beam position at the sample position (focal point) plotted against the energy of the beam. It can be seen that the deviation is kept to less than 40 mm in the frequently used energy range (9-13 keV).

The characteristics of the beam at the sample position are summarized in Table 3. The energy resolution of the beam was estimated from the full-width at half-maximum of the rocking curve with Si(111). The beam size was measured by silt scanning with a 200 μm window. The beam intensity was estimated using a PIN photo-diode to be higher than 10^{11} photons/s at the sample position, with 200 × 200 μm slit and 0.5 mrad beam divergence. Expected values calculated using ray-tracing techniques are also shown in the table, and show reasonable agreement to the measured parameters.

Table 3
Characteristics of the beam.

	Measured	Simulated
ΔE/E at 12.7 keV	2.5×10^{-4}	1.48×10^{-4}
Beam size at sample position (μm)	1.4(H) 0.18(V)	1.469(H) 0.226(V)
Photons/s at sample position (through 0.2 mm square slit)	2.0×10^{11}	5.5×10^{11}

References

[1] *Photon Factory Activity Report* **2001 #19** (2003) A60.

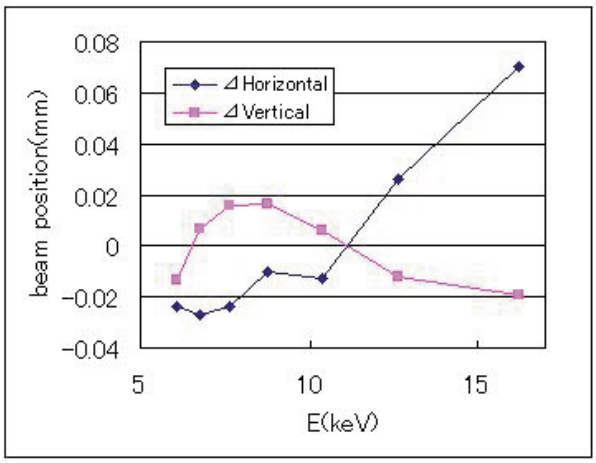

Figure 8
Deviation of the beam position at the focal point against the photon energy.